AN ASSESSMENT OF AIRCRAFT CONTROL VIA SISO CONTROL LOOPS AND TOTAL ENERGY CONTROL

H. Spark*, P. J. González†, C. Ruwisch *, W. Meyer-Brügel * and F. J. Silvestre*
* Technische Universität Berlin (TUB), Department of Flight Mechanics, Flight Control and Aeroelasticity, Marchstrasse 12, 10587, Berlin, Deutschland.
† Deutsches Zentrum für Luft- und Raumfahrt (DLR), Institut für Aeroelastik, 37073, Göttingen, Deutschland.

Abstract

The Total Energy Control System (TECS) has been proposed as an alternative control concept to track both altitude and speed in longitudinal flight. In TECS, the total energy, which is the sum of kinetic and potential energy, and the distribution between those two forms of energy is controlled. A combination of throttle and elevator input overcomes some limitations of conventional proportional-integral (PI) controllers by improving model independence of the design and considering the flight mechanical coupling between altitude and speed dynamics in the formulation. The aim of this paper is to establish a comparison between both control approaches focusing on tracking precision, disturbance rejection and transient response. To this end, a case study was evaluated using the Vitesse model aircraft as testbed. Simulation results of a closed-loop numerical model of the Vitesse with both control approaches are presented. The numerical model of the Vitesse is generated using OpenVSP and VSPAero. To find the control gains for both control approaches, the same design criteria are applied for both PI- and TECS control architectures. Results showed that both control systems are able to attain the design requirements. The velocity and altitude tracking is satisfactory. However, TECS is able to track the references with lower overshoot and lower control activity.

Keywords

TECS, PI, Flight Control, Flight Dynamics Simulation

NOMENCLATURE

Symbols

A,B,C	state matrix, input and output matrices of state-space system	
α	angle of attack	deg
BW	bandwidth	rad/s
E	total energy	J
η	elevator control surface deflection	deg
δF	throttle input	
g	acceleration due to gravity	m/s^2
γ	flight path angle	rad
GM	gain margin	dB
H	altitude	m
L	Lagrangian	J
m	mass	Kg
n_z	vertical load factor	
PM	phase margin	deg
q	pitch rate	dps
Θ	pitch angle	deg
u_K,v_K,w_K	translational velocities along the x,y,z axes	m/s
V	airspeed	m/s
x,u,y	state vector, control vector and output vector	

Indexes

cmd	command
IE	specific total energy rate error integral
IL	energy distribution error integral
kin	kinetic
PL	proportional flight path angle
pot	potential
sp	setpoint
s	specific

doi: 10.25967/550216

Abbreviations

CG	center of gravity
CRRCSim	Charles River Radio Control Flight Simulator
MIMO	multiple-Input Multiple-Output
OpenVSP	Open Vehicle Sketch Pad
PI	proportional Integral
SISO	single-input single-output
TECS	total energy control system
VLM	vortex lattice method

1. INTRODUCTION

For the selection of an altitude and speed control structure, in general aviation multiple options are available. Classically, the altitude and speed control functions are provided by pitch autopilots and autothrottle controllers [1–4]. Although in refs. [3,4], speed modes are described that do use the elevator, e.g. constant mach climb mode and level change mode, the control allocation is mostly using throttle for airspeed control (autothrottle) and the elevator for altitude control. This is based on the initial reaction of airspeed and velocity due to commands on both control inputs [3], and also the level of activity of the motor, which should be in the lower frequency range to improve its lifetime. A proportional-integral (PI) controller structure adapted to separated pitch autopilot and autothrottle loops is often employed. Hence the separated autopilot and autothrottle loops are of the type single-input and single-output (SISO).

Efficiency and performance improvement due to ecologic constraints is one of the main challenges in the aircraft industry. Possible benefits from an energy-based approach to the altitude and speed control are related to this goal. The energy-based approach has the objective to minimize elevator and throttle activity and take advantage of the aircraft's energy state by trading in speed and altitude as a pilot would [1]. The control activity reduction through TECS is highlighted in ref. [5] together with increased simulation speed in optimisation applications with 6 degree-of-freedom (6DOF) models. Other advantages of the energy-based TECS approach as increased model independence as expressed by the ability to use the same controller on different aircraft and reduced design complexity are comprehensively described in the works by Lambregts [1,6–9].

Reference [2] features a comparison of TECS and the PI structure for altitude and speed control wherein the rise time was the design criterion. A bad step disturbance rejection is attributed to the PI control structure, as it does not account for the coupling in the altitude and speed dynamics. In contrast, the authors remark that an energy-based control approach (TECS) does not show this unwanted behaviour. Moreover, with the classical linear TECS formulation they observed oscillations of the speed value in altitude step tracking-commands and vice versa.

However, some step disturbance responses in TECS-based control are based on energy exchange and therefore inherent to the TECS formulation, e.g. TECS is expected to command a nose-down/up as response to an acceleration/deceleration command [10]. For the TECS, a controller structure based on a flight-test-proven controller from [11] is used instead of the so called original structure in [2]. In the latter TECS formulation, control errors are compensated with proportional and integral control and the controlled variables used in the TECS formulation are fed back with proportional control. Those TECS control errors and variables will be introduced in Sec. 3. With this architecture, the TECS in ref. [2] is similar to the formulation of Lambregts [6]. The structure used in this work, as derived in ref. [11], changes the proportional feedback paths in TECS in comparision to the aforementioned authors. This modifications are detailed in Sec. 3.

A comparison between this TECS control structure and the PI structure is the new contribution of this work. In the comparison, one set of requirements is used to tune both controllers, TECS and PI. This work introduces the tuning methodology for the TECS controller and evaluates the difference in the effort for the controller tuning. Both controllers are implemented on the a Pixhawk 4 mini, using the PX4 flightstack as a foundation. The basic PX4 flightstack source code is publicly available to contribute to the open source community and expand the selection of controllers for this platform. In terms of ecologic efficiency, this paper aims to compare the control actuation demand of both controllers. This contribution evaluates the overall performance of PI and TECS controllers using the Vitesse motor glider model aircraft as a test case, for which a fast methodology to derive a model for the purpose of model based design is introduced in the following Section.

2. FLIGHT DYNAMICS MODEL

The comparison study on the control strategies is evaluated using the TU-Berlin fast flight dynamic model. This is a simplified flight dynamic simulation model based on the high precision flight simulator in ref. [12]. It is capable of simulating the rigid body equations of motion without the inclusion of actuators dynamics nor sensor modelling. The input file for this flight dynamics simulator consist on a stability derivatives file and a mass and inertia file.

The generation of the flight dynamic model requires the dimensions of the aircraft. The aircraft's manual states the airfoil type of the wings, the airfoil coordinates of the stabilizers were measured [13]. The mass of the fully equipped aircraft is taken and the inertia tensor components are obtained from a similar model of the aircraft included on CRRCSim [14].

Based on those dimensions of the vehicle, the geometry was modeled in OpenVSP. OpenVSP is a conceptual aircraft-design toolbox that is used to design and model a great variety of airplanes [15]. This parametric geometry

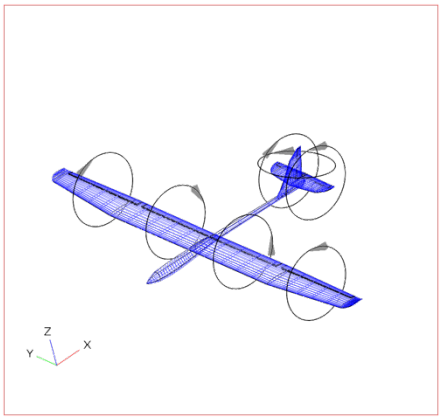

FIG 1. Vitesse geometry and panel discretisation in OpenVSP

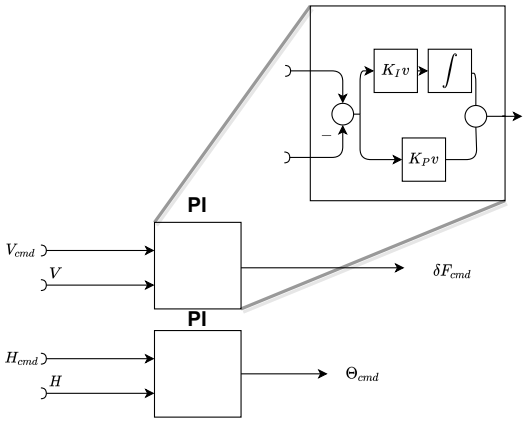

FIG 2. PI controller structure

modeler has different building capabilities that allow the operator to include main lifting surfaces, fuselages, pods, and power units in the model. At the same time, this toolbox is able to generate aerodynamic models based on the Vortex Lattice Method (VLM). The VLM engine inside OpenVSP is called VSPAERO. This software allows to build fast linear VLM models. In VSPAERO, the discrete vortices of the model are build based on the panels generated by OpenVSP and the entire surface is evaluated to obtain forces and moments. Different studies have proven that aerodynamic analyses done with OpenVSP have a good correlation with other VLM programs and experimental results [15], [16].
VSPAERO also allows the calculation of all stability and control derivatives. The derivatives are calculated using the difference between a base set of values and the solution of small step variations in the angle of attack, sideslip angles, all angular rates, and control surface deflection [17]. The OpenVSP geometry and panel discretisation of the Vitesse V2 glider is shown in Fig. 1.
The output file from OpenVSP needs to be rotated from its specific reference frame (as shown in Fig. 1) to the body-fixed reference frame, as defined in [3]. Once the derivatives are transformed to the proper orientation the flight dynamic model is built. The program allows to numerically trim the aircraft and to generate nonlinear models of the vehicle at different envelope points. These models can be linearized to design and evaluate different flight control laws in different flight conditions.

3. CONTROL STRATEGIES

This section describes the controller structures for altitude and speed control.

3.1. Proportional-integral control strategy

The authors of ref. [3] suggest the PI structure for cascaded loop control if stationary precision is needed. Also a PID structure is proposed as a standard structure for altitude and speed control. Nevertheless, the PI approach was used by ref. [4] and ref. [18] for altitude control. Also ref. [18] and ref. [19] propose the PI structure for the speed control loop. Therefore, PI control is chosen as SISO approach in this study, also enabling the comparison to the conclusions of ref. [2]. Care must be taken adding integration in the velocity loop when a non-minimal phase zero is present in the transfer function from the thrust to the velocity, which results from a motor action line below the CG. [3]. As control allocation selection, the throttle is chosen as input variable for speed control due to its more direct effect on speed and superior phugoid damping compared to an elevator-based control approach [3]. Analysis of the transfer function from thrust input to velocity response determines all zeros and poles in the left plane. So, the transfer function is minimum phase and integration in the PI speed loop is acceptable. The elevator was chosen for altitude control resulting in the same control allocation of ref. [2].
In PI control, the tracking error e, defined by command (cmd) value minus actual value, is sent to a proportional (P) gain factor and in parallel to an integral (I) gain. The sum of the error times these gains becomes the command (cmd) to an inner-loop or directly to an actuator, see Fig. 2. The following equations give the PI control loops:

$$\delta F_{cmd} = K_{Pv} e_V + K_{IV} \int e_v dT \tag{1}$$

$$\Theta_{cmd} = K_{PH} e_H + K_{IH} \int e_H dT \tag{2}$$

Reference [3] highlights the need for an inner-loop feedback of climb rate $\dot{H}$ or path angle γ to improve stability when using an integrator in the altitude control law. This inner-loop feedback is also applied in ref. [19]. To analyse and compare the control structure in ref. [2], height-rate feedback is ignored, resulting in the structure in Fig 2.
Further restrictions to a simple design in the altitude control apply in a nonlinear case. Large control errors can lead to controller actuator saturation or envelope violations. In this case a reference governor may be required [3], [20]. Some examples of these limits include:

- Height difference has to be limited to a value that relates to a pitch angle boundary,
- Load factor $n_z \sim \ddot{H}$ has to be limited for envelope protection,
- The climb rate $\dot{H}$ has to be limited to aircraft performance.

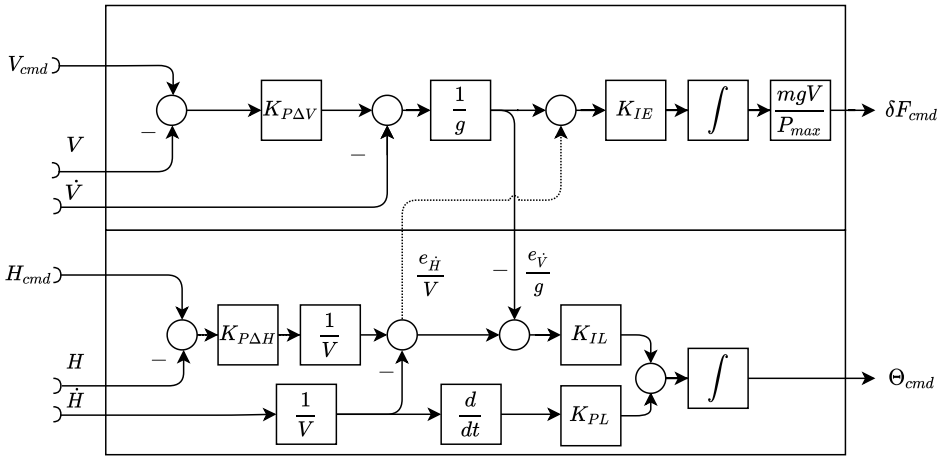

FIG 3. Simplified TECS

To avoid violating these limitations, in this study small step variations in altitude and speed are commanded. Furthermore, the aircraft model is remotely controlled and has a high control effectivity as demonstrated by the input matrix B in the Appendix. Therefore, no limitations to the simple PI design are enforced in the simulation study.

3.2. Total Energy Control System

The Total Energy Control System (TECS) is a MIMO control law based on energy exchange principles. TECS decouples flight path and speed control loops which avoids the deficiencies of SISO control with separated control loops for altitude and speed as described in [3].
This is achieved by control of the aircraft's total energy and the energy exchange between acceleration and flight path angle [1].
The total energy of an object with the mass m as sum of potential energy under the gravitational acceleration g and the kinetic energy with the speed V is

$$E = mgH + \frac{1}{2}mV^2 \ , \tag{3}$$

so the total energy rate is

$$\dot{E} = mg\dot{H} + mV\dot{V} \ . \tag{4}$$

Dividing the energy rate by mgV gives the non-dimensional specific energy rate that is controlled using throttle

$$\dot{E}_s = \frac{\dot{E}}{mgV} = \frac{\dot{H}}{V} + \frac{\dot{V}}{g} \approx \gamma + \frac{\dot{V}}{g} \ . \tag{5}$$

Wherein the small-angle approximation is done for the flight path angle γ, which can be estimated as $\frac{\dot{H}}{V}$ [21]. Defining the Lagrangian L as

$$L = E_{kin} - E_{pot} \ , \tag{6}$$

then the derivative $\dot{L}$

$$\dot{L} = \dot{E}_{kin} - \dot{E}_{pot} \tag{7}$$

is zero for conservation of the total energy. Since the energy balance can only be changed by changing the thrust setting, elevator deflections produce energy redistribution with an assumed energy rate of zero,

$$\dot{E}_s = 0 = \gamma + \frac{\dot{V}}{g} \ . \tag{8}$$

Therefore, the elevator η, assumed to not influence the total energy, is used to control the rate of energy transfer $\dot{L}$ in terms of the flight path and speed and the division by mgV is again applied to give the specific energy transfer rate $\dot{L}_s$ in Eq. 9, as in refs [21, 22]:

$$\dot{L}_s = -\gamma + \frac{\dot{V}}{g} \sim \eta \tag{9}$$

Simultaneous control of the specific energy distribution rate $\dot{L}_s$ and the specific total energy rate $\dot{E}_s$ aims at decoupling the longitudinal speed and flight path control while minimizing elevator and throttle activity. [1]
The TECS formulation used in this study is based on a modified approach by Lamp [11] in comparison to the classical TECS formulation by Lambregts [6].
In summary, the modifications of ref. [11] are:

- The use of pure integral control instead of PI control in the control path of the non-dimensional specific energy rate to achieve smoother throttle control;
- The use of only the flight path angle γ in the proportional path of the specific energy distribution rate $\dot{L}_s$, instead of full proportional feedback of $\dot{L}_s$ as defined in Eq. 9. This results in a better behaviour in turbulent air, as velocity changes will not directly affect the command value for the pitch angle;
- In this proportional path of the specific energy distribution, the value of γ is first differentiated and then integrated, see Fig. 3. This change keeps the proportional control untouched and smoothens the resultant commanded pitch angle for the inner loop.

TECS architecture has been observed to work with different aircraft models without modification of gains [23] and a TECS structure is used as a standard architecture in PX4 flightstack for fixed-wing aircraft control. In this study, the TECS controller structure is given by Fig. 3.

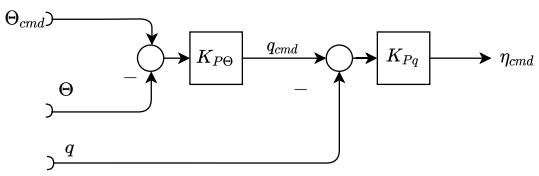

FIG 4. Pitch controller structure

To allow for a fair comparison, both the PI and the TECS controller build upon the identical pitch controller. The structure of the pitch controller is a proportional pitch angle (Θ) loop on with a proportional pitch rate (q) inner-loop, see Fig. 4.

3.3. Control Requirements

In this study, the term *requirement* is used as a synonym to the term *detailed design criterion*. The requirement definition starts with a system analysis to define goals that are reachable considering the unaugmented aircraft performance. The aircraft is well damped in the short period and the phugoid exhibits a low damping. The elevator and the motor have a high influence on the longitudinal control of the aircraft, see the input matrix (B) in the Appendix.
Based on this system analysis, the requirements for gain margin (GM) and phase margin (PM) are selected to fulfill the boundaries of the SAE94900 [24] for frequencies below the aeroelastic modes which are GM > 6 dB and PM> 45 deg. As no gain scheduling is planned, the gain margin is increased to 9.5 dB to compensate for deviating the trim conditions. The relation between gain margin and gain scheduling is emphasised in ref. [19].
The pitch damping is constrained to the limits of MIL-F-8785C [25]. As the unaugmented aircraft exhibited good pitch damping, the minimal pitch damping ratio with the pitch controller loops closed is required to be above 0.7. The bandwidths of the control channels are selected above 1.2 rad/s for the pitch and higher than 0.3 rad/s for the airspeed and altitude control, based on the need to separate the bandwidth of internal and external loops by a factor of two for a damping of 0.7 as described in [11]. Brockhaus et al. [3] also state the need for frequency separation in cascaded systems. Ref. [26] states how the phase of the plant has to be considered in selecting the bandwidth for cascaded loops. Ref. [11] calculates an example with cascaded PT1 loops and comes to the conclusion, that for unity damping the outer loop has to be four times slower than the inner loop. In comparison to this bandwidth separation factor of four, the bandwidth separation criterion is relaxed to enable lower gains in the pitch loop, see Sec. 3.4. The design requirements are summarized in Tab. 1.

3.4. Controller Tuning

A reduced state space representation of the trimmed and linearized aircraft is used for controller tuning, given by

$$\dot{x} = Ax + Bu \ , \tag{10}$$

$$y = Cx + Du \ . \tag{11}$$

The matrices A (state matrix), B (input matrix), C (output matrix) and D (feedthrough matrix) are given in the appendix for a trim point of a horizontal flight at 18 m/s and 50 m height above ground which relates to 300 m altitude above mean sea level in the present example. The state vector x of the linear model is defined as

$$x = [\quad \alpha \quad V \quad q \quad \theta \quad]^T \ , \tag{12}$$

although the variables here mean the variations with respect to their nominal values at the trim point. The aircraft model has five control inputs; elevator, motor, flaps, ailerons and rudder. In case of longitudinal controller design, the input vector u is given by:

$$u = [\quad \eta \quad \delta F \quad] , \tag{13}$$

where η is the elevator deflection and δF is the throttle input.
The state vector, Eq. 12, used for the controller tuning is selected according to ref. [4]. Note that the manoeuvres are simulated with the trim points at 15 or 20.5 m/s, see Sec. 4. For the design, the elevator actuator model of ref. [4] was added to the plant, which is a simple-lag with the time constant 0.1 s.
Since the pitch controller structure is simple, the design is done classically, with root locus analysis combined with Nichols chart evaluation of closed loop bandwidth and open loop margins. The margins are defined by the intersections of frequency response and the horizontal and vertical lines in the Nichols chart in Fig. 5.
In addition, up to ten criteria (*Crit 1* - *Crit 10*), as the pitch loop damping (`PitDmp`), pitch loop gain margin (`PitGM`), phase margin (`PitPM`), closed loop bandwidth (`PitBW`) and maximum elevator response (`PitEta`) are analysed with a self-developed linear system testing tool `lintestBench`. This tool lists the criteria imposed on one control loop and their satisfaction. The requirements are defined with soft (good to have) and hard target (mandatory) values by the designer. Bars display if the hard target is satisfied when the bar is in the *adequate* area, see Fig. 5.
Soft target satisfaction is not mandatory. The better a soft target is attained, the lower to the bottom line, labelled *best*, the bars are. Oftentimes, improving one requirement results in less satisfaction of another. This so called waterbed effect can be easily identified using the visualisation in `lintestBench` and a compromise can be found adapting the weighting factors of the gains calculation method. For the definition of the gains in the PI-Controller (see Fig. 2), the H_∞ method is used. For that, the MATLAB routine `looptune` is used to perform optimisation based on frequency criteria. The frequency-domain criteria are given in form of sensitivity and co-

TAB 1. Control requirements

Channel	Structure	Required
Pitch attitude	Proportional with inner pitch rate loop	Damping ratio $>$ 0.7 GM $>$ 9.5 dB, PM $>$ 45 deg Closed loop BW $>$ 1.2 rad/s Elevator $<$ 1 deg for unity step
Airspeed control	PI or TECS	Damping ratio $>$ 0.5 GM $>$ 9.5 dB, PM $>$ 45 deg Closed loop BW $>$ 0.3 rad/s
Altitude control	PI or TECS	Damping ratio $>$ 0.5 GM $>$ 9.5 dB, PM $>$ 45 deg Closed loop BW $>$ 0.3 rad/s

sensitivity demands. MATLAB allows to conveniently specify requirements in an application-oriented manner. Herein, the tracking bandwidth and maximum steady state error are specified. These application-oriented requirements are translated to weighting functions on the complementary sensitivity. The translation of requirements to weighting functions used for shaping the transfer functions is an arduous process. Some application examples are available in [27] and [28], both based on the work of Apkarian, Noll and Gahinet [29, 30].

Besides satisfying the requirements of Tab. 1, the bandwidth and damping of the PI system should be close to the TECS system for a fair comparability. Not all requirements of Tab. 1 are defined in the `looptune` optimisation. In fact, a combination of using these and the visualisation in `lintestBench` was applied instead.

The definition of the gains in the TECS controller in Fig. 3 is accomplished with gridding. First, the innermost gains – K_{IE} for the specific total energy rate error integral gain, K_{IL} for the energy *distribution* error integral gain and K_{PL} for the proportional flight path angle gain – are varied.

One restriction, that K_{IE} shall equal K_{IL}, is applied to simplify the design. Further, it is considered to be optimal to reach identical dynamics in energy rate error $\dot{E}_e$ and energy distribution rate error $\dot{L}_e$ as required by ref. [31].

After varying n times $K_I(= K_{IE}, K_{IL})$ and n times K_{PL}, the resultant grid of n^2 TECS controllers is generated, and a coupling of each combination to the lower cascades (pitch controller and plant) is accomplished.

The resultant n^2 systems $\dot{V}_{cmd} \rightarrow \dot{V}$ and $\dot{H}_{cmd} \rightarrow \dot{H}$ are analysed for bandwidth and damping. Based on the following final criteria a set of gains is selected from the grid:

- Bandwidth separation 1: The maximum bandwidth of the TECS loops should be less than half of the pitch loop;
- Bandwidth separation 2: The TECS bandwidth shall be at least two times the desired bandwidth of the respective outer speed and altitude loops;
- The damping of the TECS loops shall be sufficiently ($\sqrt{2}$ times) greater than the desired damping for the outer speed and altitude loops.

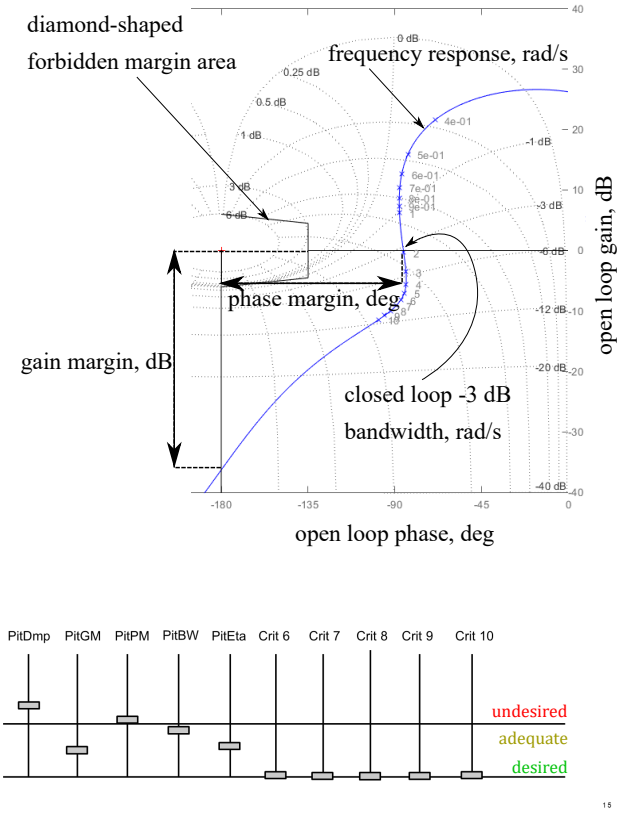

FIG 5. Design tools Nichols margin plot and `lintestBench`

In the absense of a model for the motor dynamics, the bandwidth criterion for the loop $\dot{V}_{cmd} \rightarrow \dot{V}$ was violated as the loop became too fast. Analysis in Sec. 5 point to an effect of this on the speed control behaviour.
After the design of the TECS gains, the speed loop is added by gridding over the proportional speed loop gain $K_{P\Delta V}$, see Fig. 3, using the same gridding criteria of bandwidth and damping and the evaluation of all requirements of Tab. 1 for the determination of the gain. The same procedure is then applied to the proportional altitude loop gain $K_{P\Delta H}$.

4. CASE OF STUDY

The case study of this research is the Vitesse V2 model aircraft. It is a composite material radio-controlled motor glider. The aircraft is shown in Fig. 6.
The glider has a span of 3 m, a fuselage length of 1.385 m, and a wing surface of 0.655 m^2. The take-off weight of the fully instrumented aircraft is 3.1 kg. The instrumentation consists of a Pixhawk 4 mini bundle with a GPS and an air data probe installed on the right wing. The system is capable to provide all angular rates, Euler angles, control commands to the motor and control surfaces, airspeed, ground speed, and position. Part of the requirements of the controllers was based on the available data of this system. Four manoeuvres are selected to identify the performance of the controllers.
For the initial assessment of the controllers, the first two manoeuvres are analysed.

- For *Manoeuvre 1*, the aircraft model was trimmed at 18 m/s and 50 m of height. From the trim point, the manoeuvre consists of an height variation step command of 10 m while keeping the velocity constant.
- For *Manoeuvre 2*, the aircraft model was trimmed at 15 m/s and 50 m of height. Manoeuvre 2 consists of a step velocity variation command of 5.5 m/s while keeping the height constant.

Thus, Manoeuvre 1 and 2 are step commands for either altitude or speed.
The following, remaining two manoeuvres include simultaneous changes in altitude and speed as in a point mass energy exchange. These energy exchange manoeuvres are based on the exchange of kinetic energy $\frac{1}{2}mV^2$ and potential energy $mg\Delta h$, see Eq. 14.

$$\frac{1}{2}mV_2^2 - \frac{1}{2}mV_1^2 = mg\Delta h \tag{14}$$

Due to stall constraints, one limitation on the manoeuvres is that the lowest commanded speed shall be 15 m/s. Another constraint is that the step response shall be clearly identifiable and separable from wind influences in later flight test. Therefore, an altitude step of 10 m is selected which relates to a speed change of 5.5 m/s by evaluation of Eq. 14.
Based on this analysis of the energy exchange, the last two manoeuvres are:

- *Manoeuvre 3* is a simultaneous change in velocity and height – from 20.5 m/s to 15 m/s and from 50 m to 60 m. Therefore, the aircraft model was trimmed at 20.5 m/s and 50 m of height.
- *Manoeuvre 4* is a simultaneous change in velocity and height from from 15 m/s to 20.5 m/s and from 50 m to 40 m. The aircraft model was trimmed at 15 m/s and 50 m of height.

Nevertheless, the gains for both control laws were designed for a flight condition of 18 m/s and 50 m. These manoeuvres will allow to observe the energy change to achieve two different steady state conditions. At the same time, the manoeuvres will help to observe the response of the different control loops to crossed reference commands and to show the difference in control actuation.

FIG 6. Vitesse V2 model

5. RESULTS

The gains have been determined for the two control laws, and are summarised in Tab. 2. In the following, the nonlinear closed-loop simulation results are analysed. The characteristics of both control approaches are assessed in terms of tracking precision, control usage and disturbance rejection, considering the manoeuvres described in the previous section.
The combination of controllers and plant result in the requirement satisfaction documented in Tab. 3.

TAB 2. Control gains

Channel	Gain	Value
Pitch	K_{Pq}	0.059
	$K_{P\theta}$	5.3
PI	K_{PV}	1.96
	K_{IV}	0.0175
	K_{PH}	2.41
	K_{IH}	0.355
TECS	K_I	0.3
	K_P	0.8
	$K_{P\Delta H}$	0.3
	$K_{P\Delta V}$	0.3

TAB 3. Control requirement results

Channel	Structure	Required
Pitch attitude	Proportional with inner pitch rate loop	Damping Ratio 0.82 GM 36 dB, PM 94 deg Closed loop BW 1.9 rad/s Elevator -0.313 deg for Unity Step
Airspeed control	TECS	Damping Ratio 0.82 GM inf dB, PM 83 deg Closed loop BW 0.38 rad/s
Airspeed control	PI	Damping Ratio 0.84 GM 54 dB, PM 89 deg Closed loop BW 0.56 rad/s
Altitude control	TECS	Damping Ratio 0.54 GM 13 dB, PM 50 deg Closed loop BW 0.45 rad/s
Altitude control	PI	Damping Ratio 0.62 GM 17 dB, PM 53 deg Closed loop BW 1.23 rad/s

Track precision and disturbance rejection

Figure 7 shows the response to Manoeuvre 1. The TECS demonstrates less overshoot of 14.8 % while the PI has an overshoot of 22.4 %. The TECS shows less velocity deviation (2.1 %), whereas the PI has a drop of 15.1 % in the velocity. Therefore, the TECS shows a better step rejection than the PI. The PI can not compensate for the energy demand of the climb and therefore exhibits bad velocity step rejection. The PI control strategy demonstrates a significantly faster altitude response with a rise time of 1.91 s as opposed to 4.37 s with TECS. This is expected by the fast PI bandwidth in Tab. 3. Still, the PI's settling time is larger.
The overall elevator and throttle activity is high with PI control. The PI exhibits a maximum elevator offset of 7.46 deg from the trim value for Manoeuvre 1. TECS demands an offset of 0.45 deg. Note, that for the controller design the elevator actuator model of [4] is used, the flight mechanical simulation however lacks any actuator models which results in a step command to the elevator in the PI control scheme as result of the step command in altitude.
Possible improvements in PI control to eliminate such behaviour are described Sec. 3.
Besides this, the throttle demand of the PI is higher with a difference of 6.01 N relative to the reference state. The TECS requires a thrust change of only 3.01 N.
As can be seen in Fig. 7, with the TECS controller, velocity is not traded in for the increasing height demand in the Manoeuvre 1 as expected. Instead, the velocity increases initially, simultaneously with height. This points to a coupling of speed and height dynamics and a non-optimal selection of dynamics in the TECS loops (see refs. [3] and [31]).
Figure 8 shows the responses to Manoeuvre 2. For the TECS, in this speed step a reasonable exchange of altitude for speed can be observed which is favourable to reduce throttle activity. The PI again shows a faster response as its bandwidth exceeds the TECS's. On the downside, the PI's throttle activity implies addition of restrictions to the simple design as described in Sec. 3. Besides this, note the step disturbance rejection. With the PI controller, the aircraft gains height as result of the increased lift and only slowly returns to the height setpoint.
The TECS on the other hand shows an energy trade to achieve a smooth step response and less throttle activity. This energy trade is not an unwanted oscillation but a result of the control strategy. In brief, the results of Manoeuvre 2 agree with the observations made for Manoeuvre 1.

Energy exchange manoeuvres

Figures 9 and 10 show the energy exchange manoeuvres. In the Manoeuvre 3, the setpoints in height and speed are tracked with a rise time of 4.36 s and 5.28 s respectively by the TECS. The TECS demonstrates negligible height overshoot of 1.4 % in and zero overshoot in the speed. The TECS's elevator activity is low with a maximum deflection delta from 0.63 deg from trim. The thrust usage is smooth for the TECS with less than half (1.11 N to 2.39 N) of thrust deviation compared to the PI. For the PI, the rise times in Manoeuvre 3 are 1.95 s in the height and 1.4 s in the velocity. The setpoints are reached with an overshoot of 7.7 % and 20.3 % for altitude and speed. The PI control activity in the elevator is high, with a difference in deflection of 7.44 deg and an instantaneous command, as seen above in the altitude step rejection response.
Figure 10 shows the same trends in Manoeuvre 4. With the PI, setpoints are reached with more overshoot and

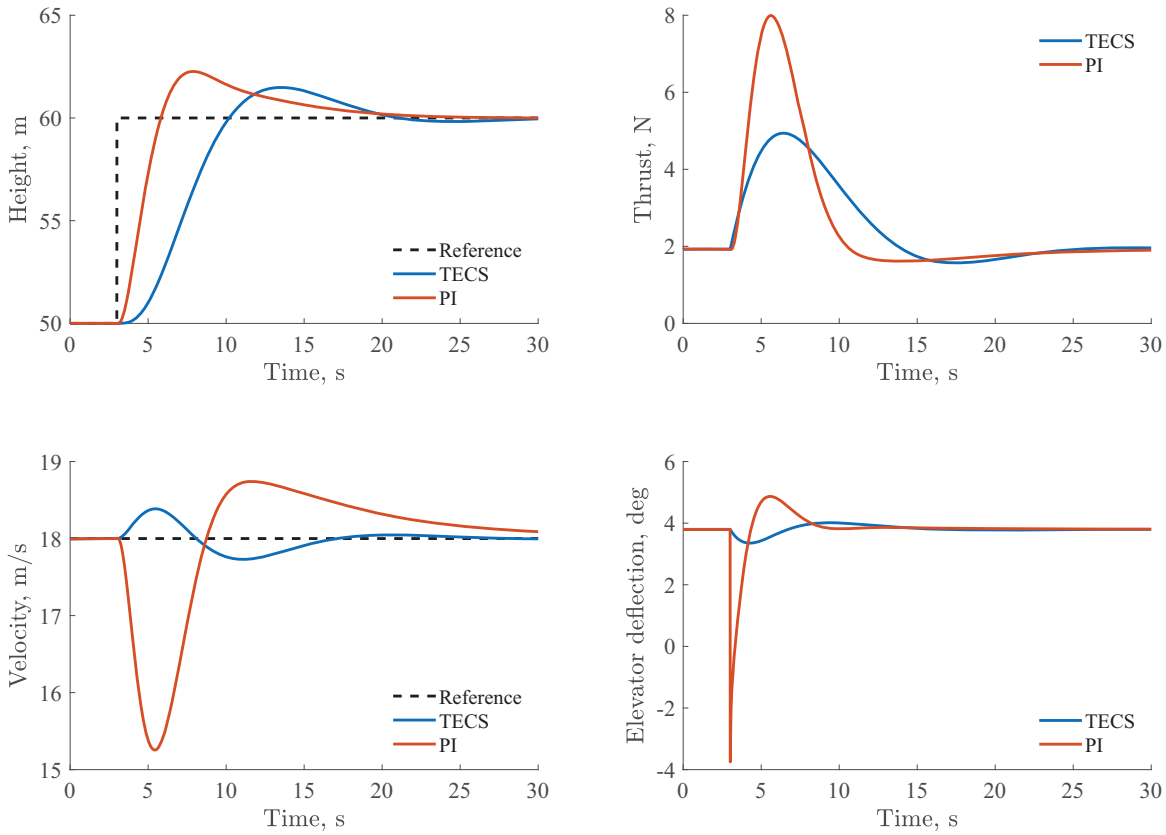

FIG 7. Manoeuvre 1: positive altitude step combined with speed hold

higher control activity, identifying the need for command shaping and/or limiting, see Sec. 3.

The energy exchange manoeuvres are calculated to be ending on the same energy level from a point mass view. The TECS thrust deviation from trim is positive at start of Manoeuvre 3, see Fig. 9 and negative in Manoeuvre 4, see Fig. 10. However, the required thrust offset from the trim thrust value at the end of those manoeuvres has a different sign than those initial responses. This offset is due changes in aircraft drag with speed, which the point mass simplification does not consider. Based on the point mass simplification, the TECS controller should not change the throttle setting initially, only slowly to compensate for new aircraft drag as the speed deviates from the trim point. The initial throttle response in another direction points to further optimisation possibilities.

These results in the throttle response suggest possibilities to improve the tuning of the TECS gains with respect to the dynamics of energy rate error control and energy distribution rate error control. The requirement of identical error rate dynamics, see ref. [31], can to be evaluated. By only setting the TECS inner loop integral gains to identical values, the resultant decoupling leaves room for improvement. As pointed out in Sec. 3.4 the speed controller dynamics are fast, and in the disturbance rejection analysis a coupling of speed and height dynamics was also observed. This can be attributed to the lack of a motor model as ref. [31] points out that the pitch attitude dynamics should be designed to match the engine dynamics which were not available. Hence, the energy rate control is faster than the energy distribution. This explains the initial acceleration response to an altitude step in Fig. 7.

6. CONCLUSION

Two longitudinal controllers for a UAV sailplane were developed. The first one is based on conventional PI control and the second one is based on TECS. Both controllers satisfy all given linear requirements. The simulated airspeed and height commands are tracked smoothly. An energy trade was observed in the TECS control that could be used to adapt to wind changes in sailplane operation. Results showed that TECS demanded lower control activity for all simulated manoeuvres. Therefore, the TECS can be suggested for energy efficient flight control.

The TECS controller gains were derived with a set of rules for both bandwidth and damping leading to simple gain gridding. This lead to less design effort than for the PI. With this TECS design, the results showed small coupling between airspeed and height. Therefore, the design criteria for the TECS should be adapted in future design. The introduced bandwidth separation criteria should be evaluated with regard to the specific energy rate dynamics and energy rate distribution dynamics. Although already exceeding the PI performance, the TECS design can thus be improved further.

The design for the PI controller resulted in a higher bandwidth and higher overshoot response than specified in the

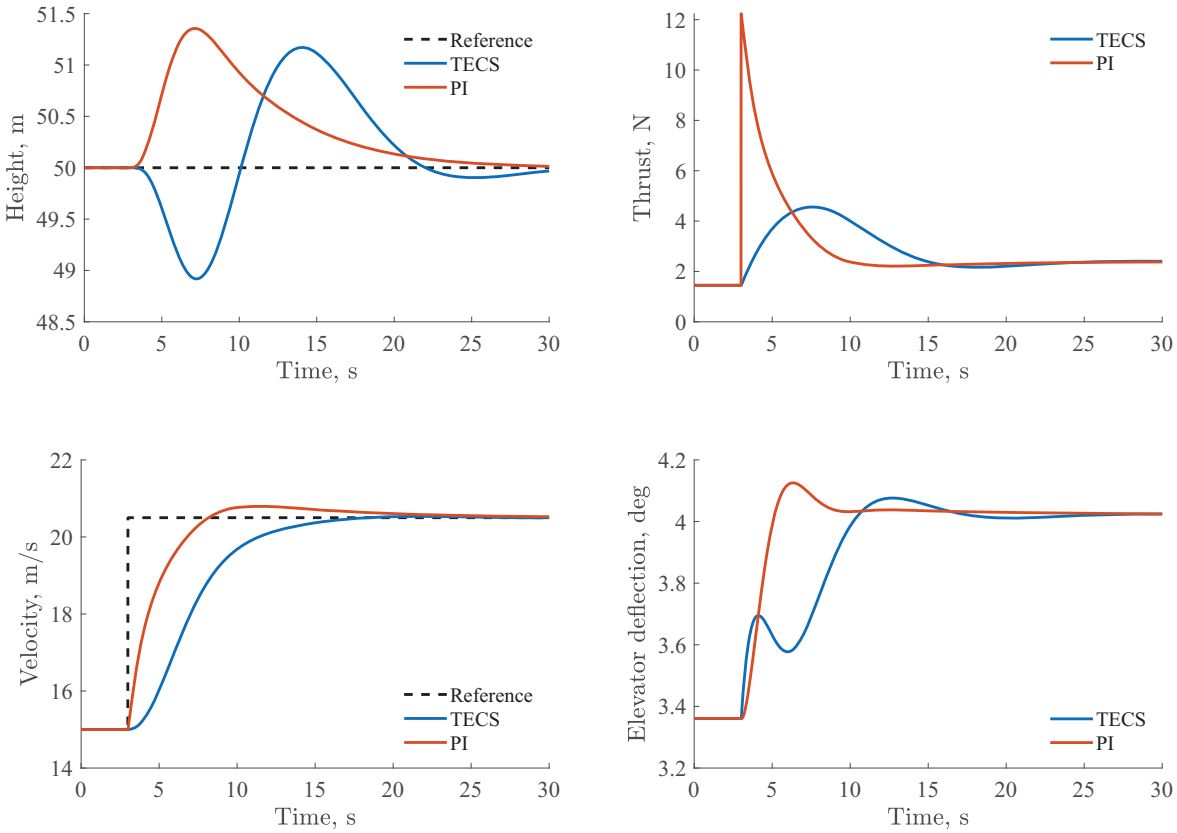

FIG 8. Manoeuvre 2: positive speed step combined with altitude hold

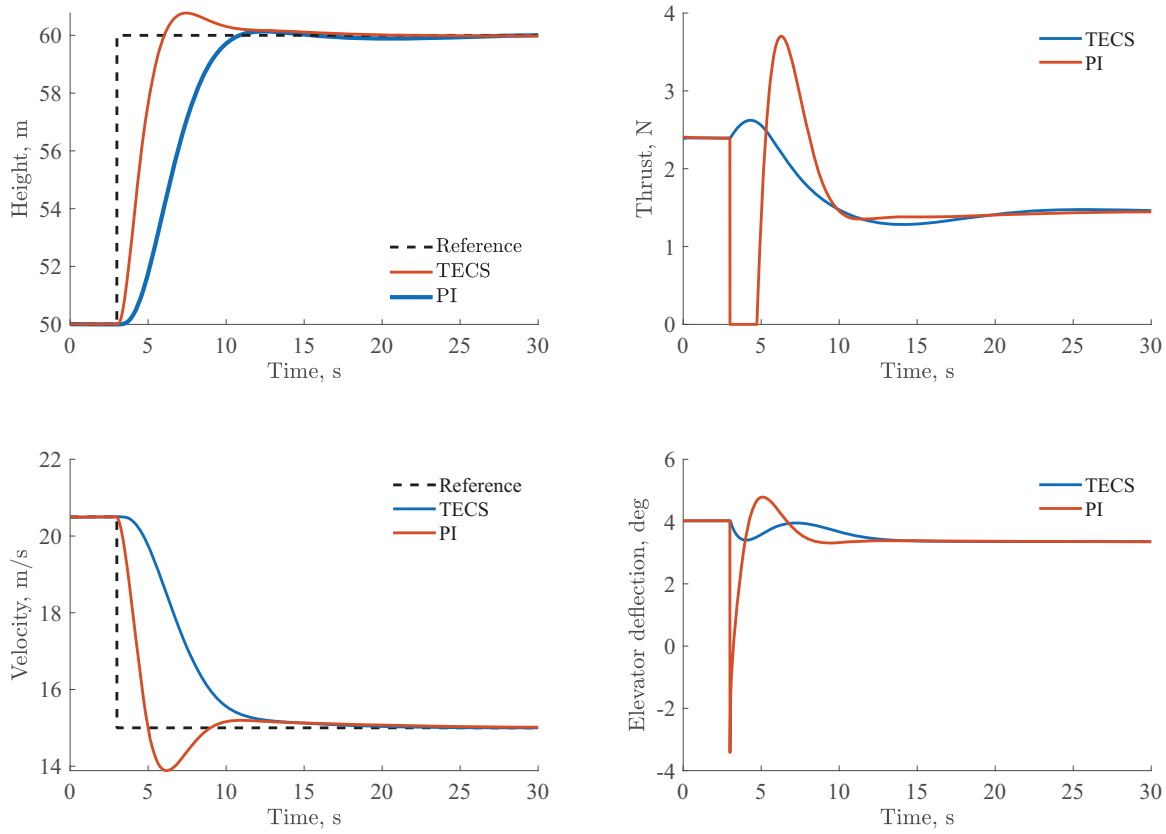

FIG 9. Manoeuvre 3: positive altitude step in manoeuvre and negative speed step in manoeuvre

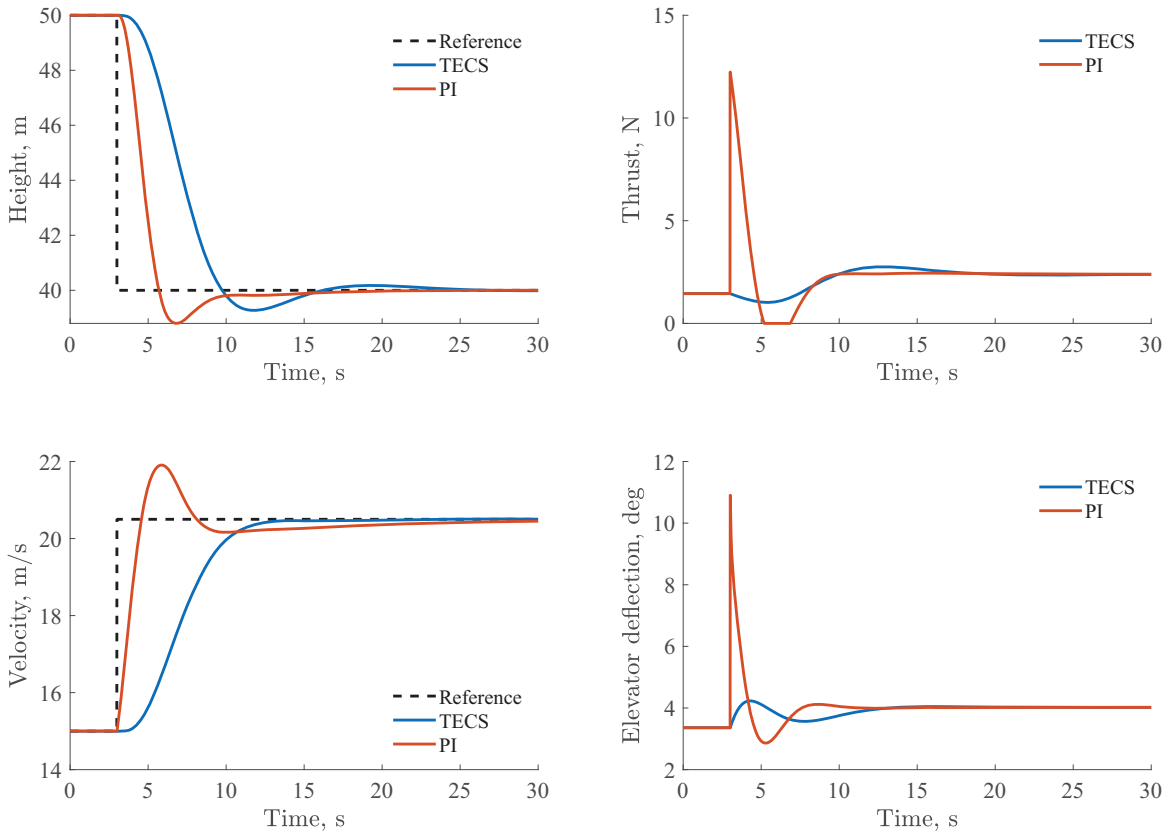

FIG 10. Manoeuvre 4: negative altitude step in manoeuvre and positive speed step in manoeuvre

`looptune` requirement inputs. To allow for a more direct comparison of both control architectures, a design process ensuring identical dynamic properties in terms of bandwidth and damping would be beneficial. Therefore, another point to be evaluated is the design flow in the PI gain optimisation. Some design metrics were a priori input to the optimiser. Other design metrics were a posteriori analysed with the tool `lintestBench`. Including all requirements in a one-shot optimisation process would be wishful. Then, the `lintestBench` can serve as a reporting and checking tool rather than a design tool. For the simple PI, restrictions in inputs and output limiters should be added for safety, even though the small input signals in this work do not necessitate them.
Future work will include flight testing the proposed controllers with the glider. The model, as produced by the FASTSim toolchain, will be evaluated and validated in flight test. Accordingly, the control laws will also be tested in-flight. On-board measurements of the energy draw will be obtained to verify simulation results on control efficiency.

Contact address:

spark@tu-berlin.de
The source code for this work is available at github: https://github.com/NuclearHenne/PX4-Autopilot

References

[1] A. A. Lambregts. Vertical flight path and speed control autopilot design using total energy principles, AIAA 83-2239. 1983. DOI: 10.2514/6.1983-2239.

[2] Matthew E. Argyle and Randal W. Beard. Nonlinear total energy control for the longitudinal dynamics of an aircraft. In American Control Conference, editor, *2016 American Control Conference (ACC)*, pages 6741–6746, [Piscataway, NJ], 2016. IEEE. `http://ieeexplore.ieee.org/document/7526733/`. DOI: 10.1109/ACC.2016.7526733.

[3] R. Brockhaus, W. Alles, and R. Luckner. *Flugregelung*. Springer, 3. edition, 2011. ISBN: 978-3-642-01442-0.

[4] B. L. Stevens, F. L. Lewis, and E. N. Johnson. *Aircraft Control and Simulation: Dynamics, Control Design, and Autonomous Systems*. Wiley, 3. edition, 2016.

[5] M. Cooper, C. Lawson, and A. Zare Shahneh. Simulating Actuator Energy Consumption for Trajectory Optimisation. In *Proceedings of the Institution of Mechanical Engineers, Part G: Journal of Aerospace Engineering*, volume 232(11), pages 2178–2192. 2018. DOI: 10.1177/0954410017710271.

[6] A. A. Lambregts. Total energy based flight control system: United states patent 4536843, 1984.

[7] Lambregts. Functional integration of vertical flight path and speed control uning energy principles. In *First Annual NASA Aircraft Controls Workshop, 1983*.

[8] A. Lambregts. Integrated system design for flight and propulsion control using total energy principles. In *Aircraft Design, Systems and Technology Meeting*, Reston, Virigina, American Institute of Aeronautics and Astronautics, 2012. DOI: 10.2514/6.1983-2561.

[9] A. A. Lambregts. Operational Aspects of the Integrated Vertical Flight Path and Speed Control System. In *SAE Technical Paper Series*, SAE Technical Paper Series. SAE International400 Commonwealth Drive, Warrendale, PA, United States, 1983. DOI: 10.4271/831420.

[10] N. Kastner and G. Looye. Generic TECS based autopilot for an electric high altitude solar powered aircraft. In *Proceedings of the EuroGNC-2013*. 2013.

[11] M. Lamp. *Automatische, schublose Landung eines Flugzeuges großer Streckung unter Verwendung der Bremsklappen und mit variablen Gleitpfadwinkeln*. Dissertation, TU Berlin, 2015.

[12] W. Meyer-Brügel. *Präzisere Echtzeit-Flugsimulation kleiner Nutzflugzeuge durch Integration feingranularer Teilmodelle: am Beispiel der Aktuator-und Fahrwerksmodellierung*. Technische Universitaet Berlin, 2019.

[13] Gustav Staufenbiel GmbH. DYMOND MODELL-SPORT - Anleitung Vitesse V2, [cited on August 2021]. https://www.horizonhobby.de/on/demandware.static/Sites-horizon-eu-Site/Sites-horizon-master/default/Manuals/HSF0314063EV2-Manual-DE.pdf.

[14] CRRCSIM. Open source model airplane simulator, [cited on August 2021]. https://sourceforge.net/projects/crrcsim/.

[15] E. Olson and C. Albertson. Aircraft High-Lift Aerodynamic Analysis Using a Surface-Vorticity Solver. In *54th AIAA Aerospace Sciences Meeting*, AIAA 2016-0779, San Diego, California, American Institute of Aeronautics and Astronautics, 2016. DOI: 10.2514/6.2016-0779.

[16] E. Olson. Semi-Empirical Prediction of Aircraft Low-Speed Aerodynamic Characteristics. In *53th AIAA Aerospace Sciences Meeting*, AIAA 2015-1679, Kissimmee, Florida, American Institute of Aeronautics and Astronautics, 2015. DOI: 10.2514/6.2015-1679.

[17] OpenVSP. Using vspaero, [cited on August 2021]. http://openvsp.org/wiki/doku.php?id=vspaerotutorial.

[18] R. W. Beard and T. W. McLain. *Small Unmanned Aircraft: Theory and Practice*. Princeton University Press, New Jersey, 2012. ISBN: 978-0-691-14921-9.

[19] W. Falkena. *Investigation of Practical Flight Control Systems for Small Aircraft*. Dissertation, Delft University of Technology, 2012.

[20] I. Kolmanovsky, E. Garone, and S. Di Cairano. Reference and Command Governors: A Tutorial on Their Theory and Automotive Applications. In *2014 American Control Conference*, pages 226–241. IEEE, 2014. DOI: 10.1109/ACC.2014.6859176.

[21] Willigen, R. J. van der. *The Total Energy Control System*. Thesis, Delft University of Technology, 1996.

[22] A. A. Lambregts. Generalized Automatic and Augmented Manual Flight Control: Berlin Technical University Colloquium May 19, 2006.

[23] G. Looye. TECS/THCS-based generic autopilot control laws for aircraft mission simulation. In *Proceedings of the EuroGNC-2013*, 2013.

[24] S. of Automotive Engineers. Aerospace Standard AS94900, flight control systems, 2007.

[25] Department of Defense. Flying Qualities of Piloted Airplane MIL-F-8785C, 1980.

[26] S. Skogestad and I. Postlethwaite. *Multivariable Feedback Control: Analysis and design*. Jon Wiley & Sons, Chichester, England, second edition edition, 2005. ISBN: 13978-0-470-01167-6.

[27] D. Ossmann, T. Luspay, and B. Vanek. Baseline Flight Control System Design for an Unmanned Flutter Demonstrator. In *IEEE Aerospace Conference 2019*. DOI: 10.1109/AERO.2019.8741853.

[28] Dezong Zhao, Edward Winward, Zhijia Yang, Richard Stobart, and Thomas Steffen. Real-Time Optimal Energy Management of Electrified Engines. *IFAC-PapersOnLine*, 49(11):251–258, 2016. DOI: 10.1016/j.ifacol.2016.08.038.

[29] P. Apkarian. Tuning controllers against multiple design requirements using constrained nonsmooth optimization, 2014. http://pierre.apkarian.free.fr/CCT_ApkaNov2014_PUBLISHED.pdf.

[30] P. Apkarian and D. Noll. Nonsmooth H-infinity Synthesis. In *IEEE Transactions on Automatic Control*, volume 51-1, pages 71–86. 2006.

[31] L. F. Faleiro and A. A. Lambregts. Analysis and tuning of a 'total energy control system' control law using eigenstructure assignment. *Aerospace Science and Technology*, 3(3):127–140, 1999. DOI: 10.1016/S1270-9638(99)80037-6.

APPENDIX

$$A = \begin{array}{c} \\ \alpha \\ V \\ q \\ \Theta \end{array} \begin{array}{c} \begin{array}{cccc} \alpha & V & q & \Theta \end{array} \\ \begin{bmatrix} -11.71 & -0.06064 & 0.7973 & 0 \\ 7.166 & -0.06892 & -0.101 & -9.81 \\ -44.75 & 0 & -17.87 & 0 \\ 0 & 0 & 1 & 0 \end{bmatrix} \end{array}$$

$$B = \begin{array}{c} \\ \alpha \\ V \\ q \\ \Theta \end{array} \begin{array}{c} \begin{array}{cc} \eta & \eta_F \end{array} \\ \begin{bmatrix} -0.01151 & 0.000405 \\ -0.005607 & 0.3225 \\ -2.144 & 0 \\ 0 & 0 \end{bmatrix} \end{array}$$

$$C = \begin{array}{c} \\ \alpha_{deg} \\ V \\ q_{dps} \\ \Theta_{deg} \end{array} \begin{array}{c} \begin{array}{cccc} \alpha & V & q & \Theta \end{array} \\ \begin{bmatrix} 57.3 & 0 & 0 & 0 \\ 0 & 1 & 0 & 0 \\ 0 & 0 & 57.3 & 0 \\ 0 & 0 & 0 & 57.3 \end{bmatrix} \end{array}$$

$$D = 0_{4,2}$$